Neuron, Volume *110*

Supplemental information

Endothelial PlexinD1 signaling instructs spinal cord vascularization and motor neuron development

José Ricardo Vieira, Bhavin Shah, Sebastian Dupraz, Isidora Paredes, Patricia Himmels, Géza Schermann, Heike Adler, Alessia Motta, Lea Gärtner, Ariadna Navarro-Aragall, Elena Ioannou, Elena Dyukova, Remy Bonnavion, Andreas Fischer, Dario Bonanomi, Frank Bradke, Christiana Ruhrberg, and Carmen Ruiz de Almodóvar

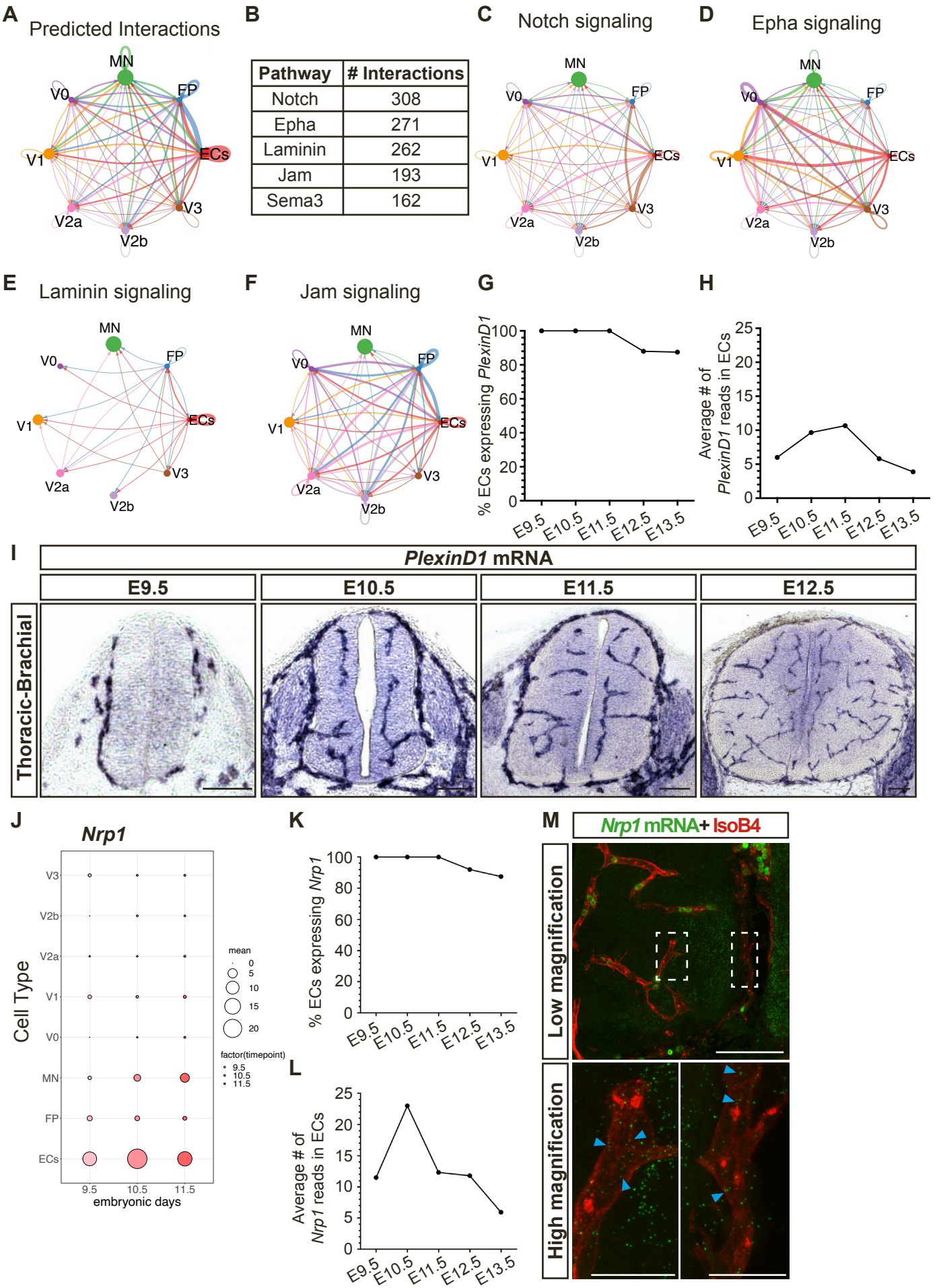

Fig. Sup. 1 - Related to Figure 1

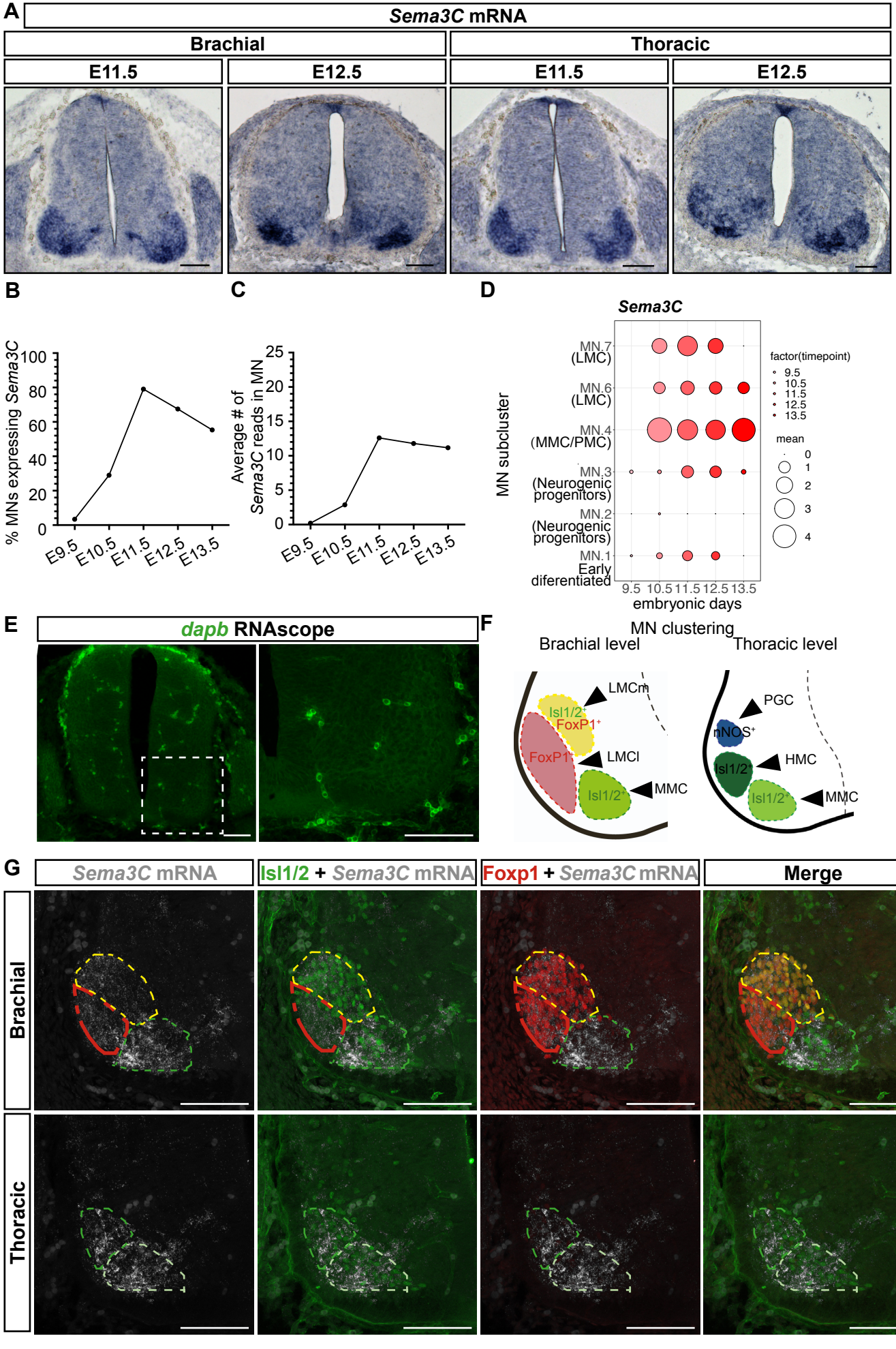

Fig. Sup. 2 - Related to Figure 1

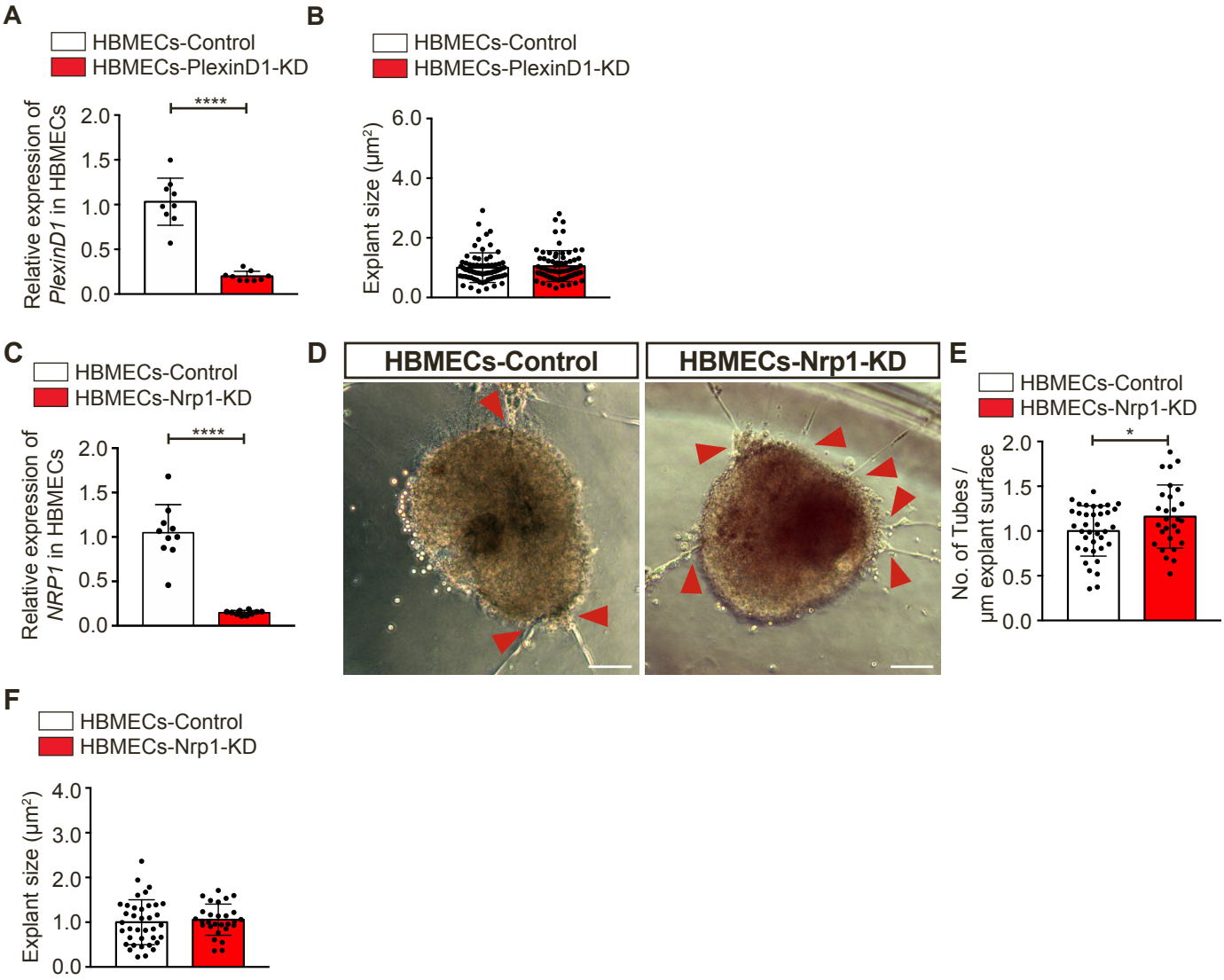

Fig. Sup. 3 - Related to Figure 2

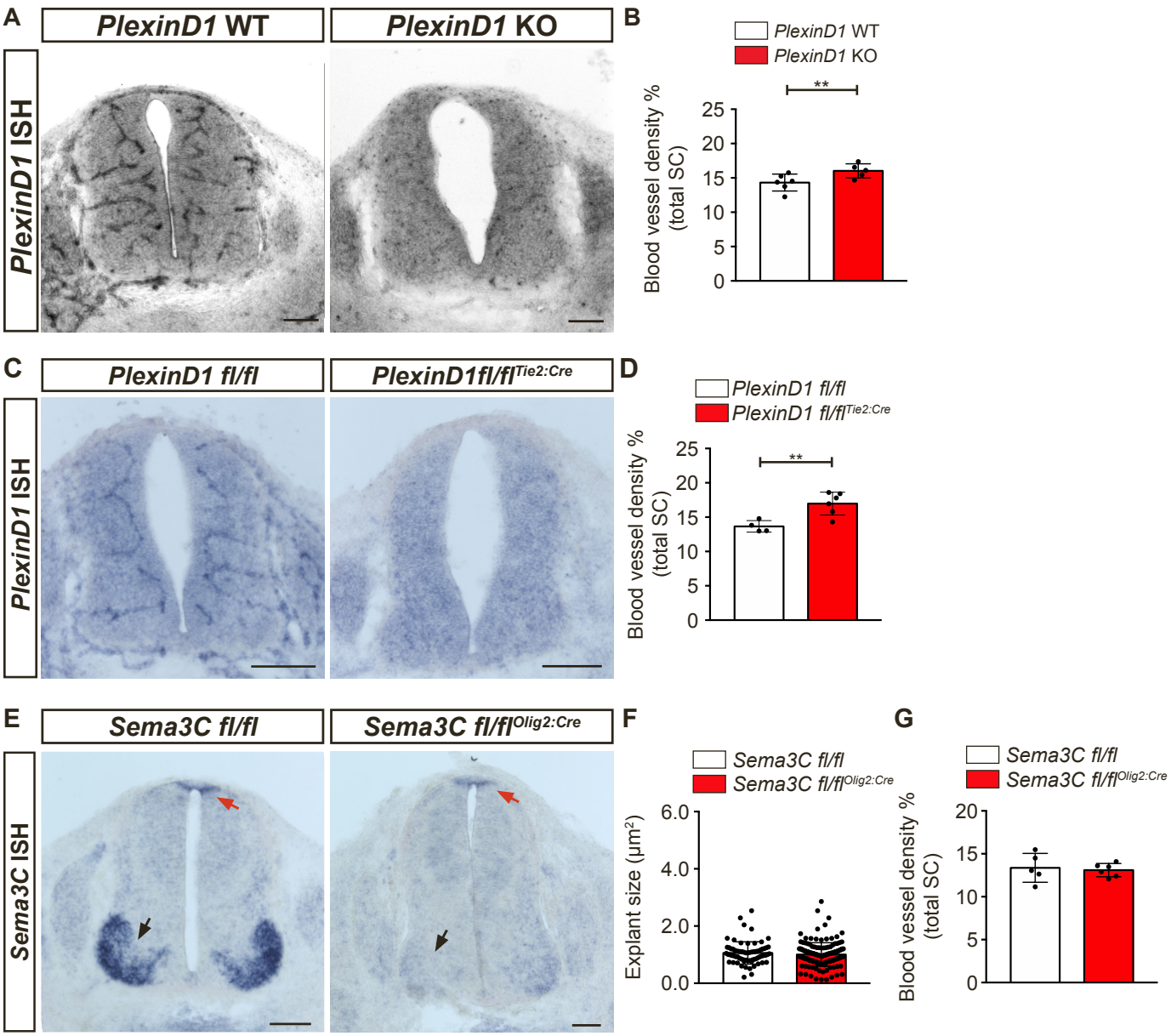

Fig. Sup. 4 - Related to Figure 2, 3 and 4

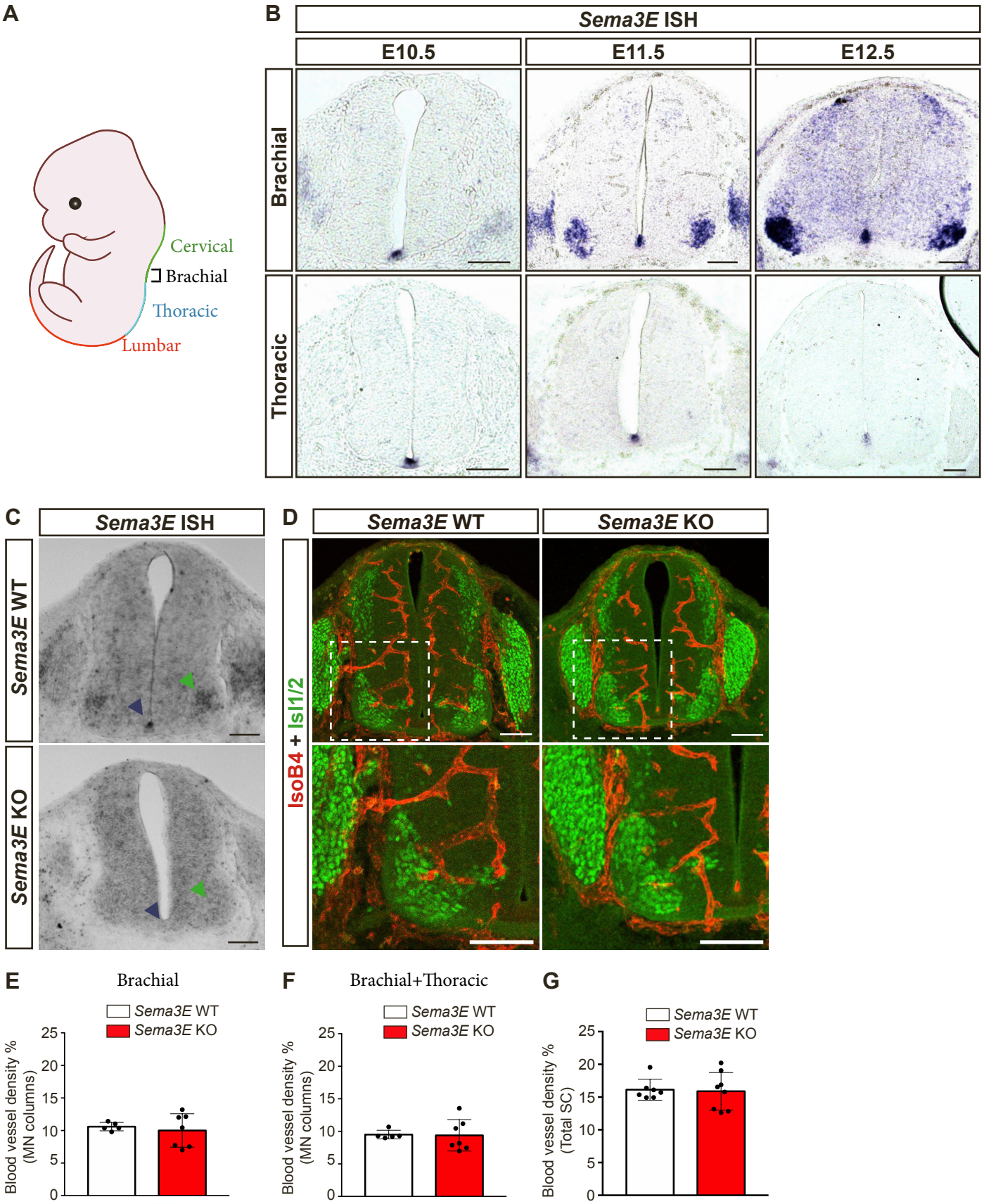

Fig. Sup. 5 - Related to Figure 4

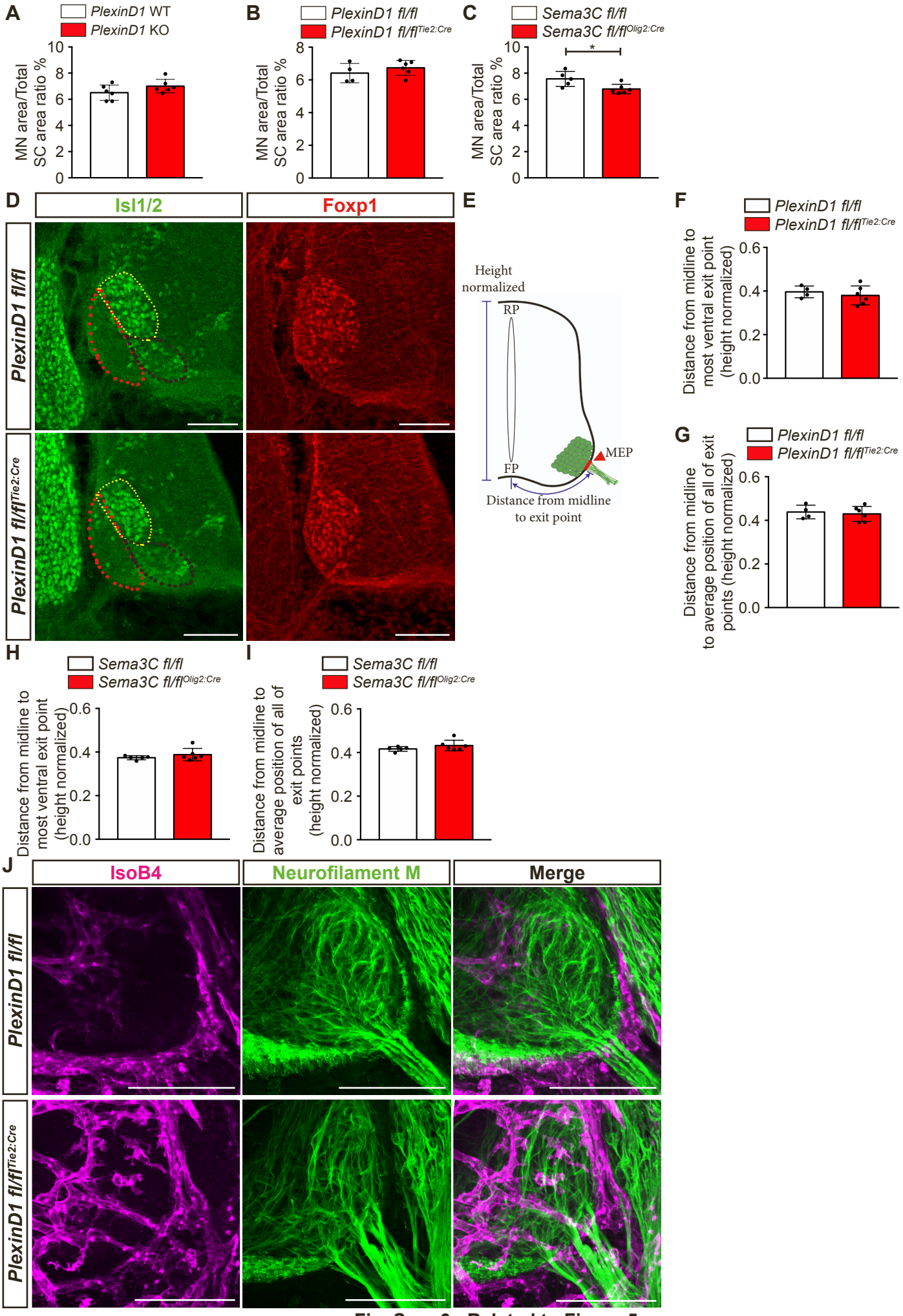

Fig. Sup. 6 - Related to Figure 5

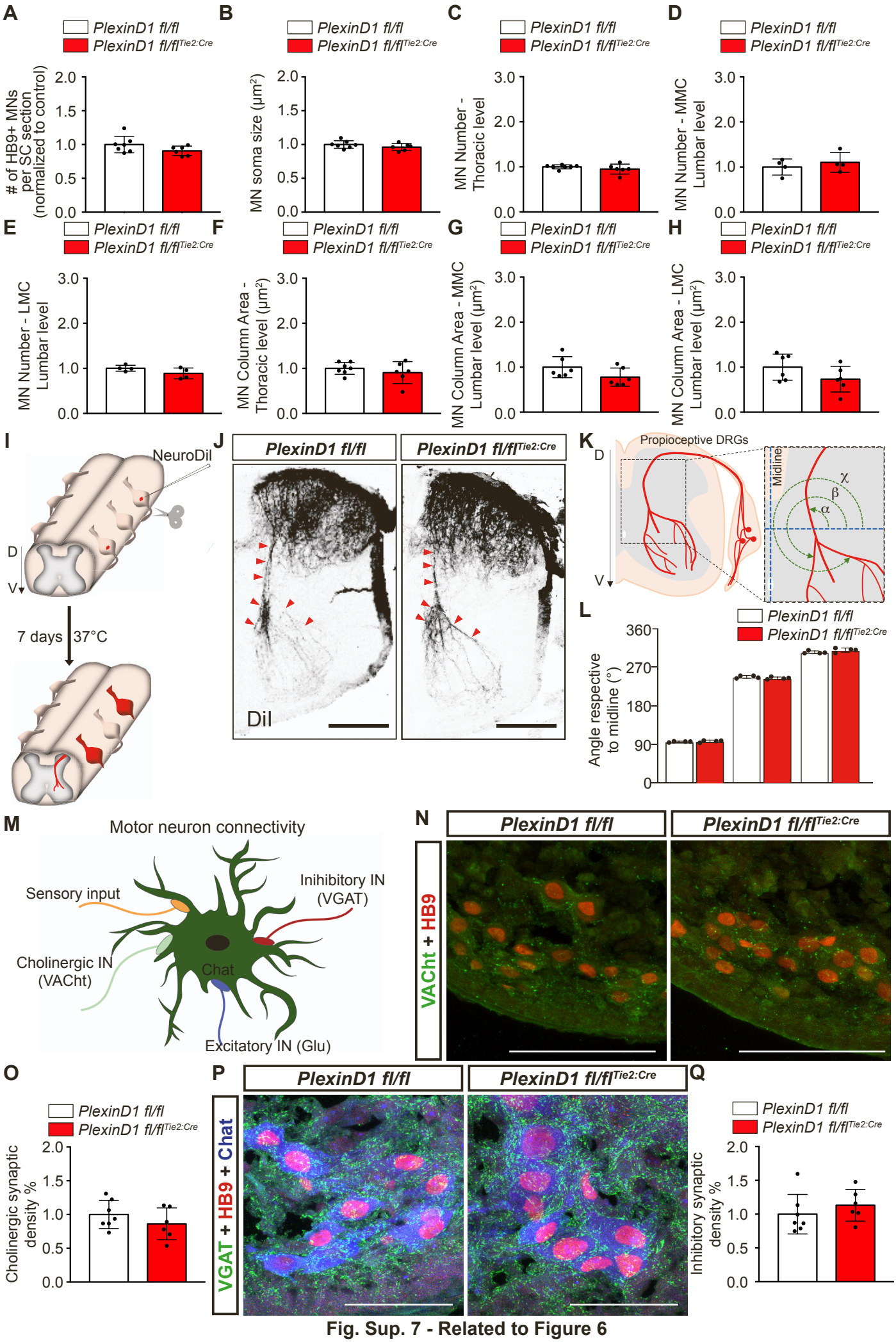

Fig. Sup. 7 - Related to Figure 6

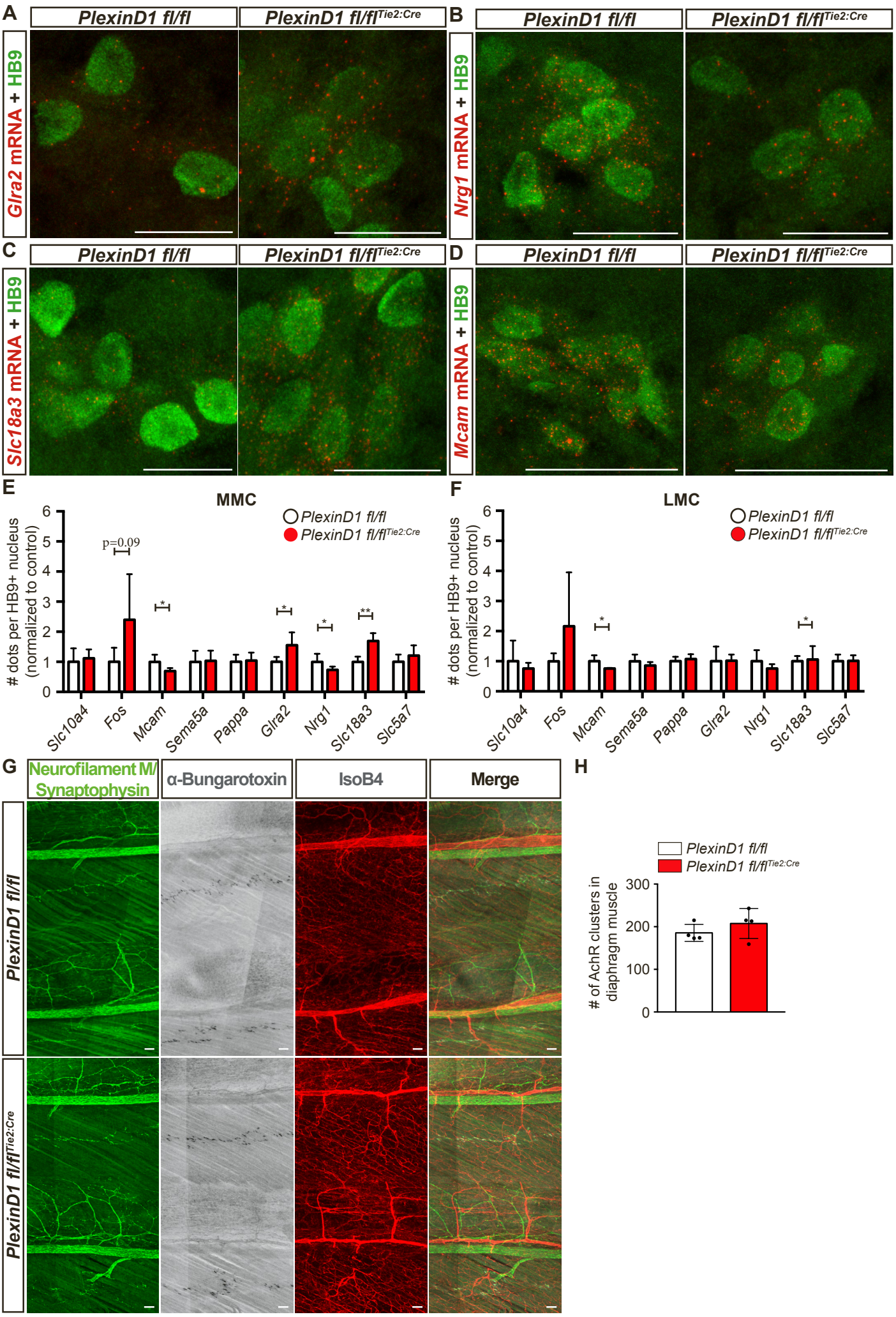

Fig. Sup. 8 - Related to Figure 6

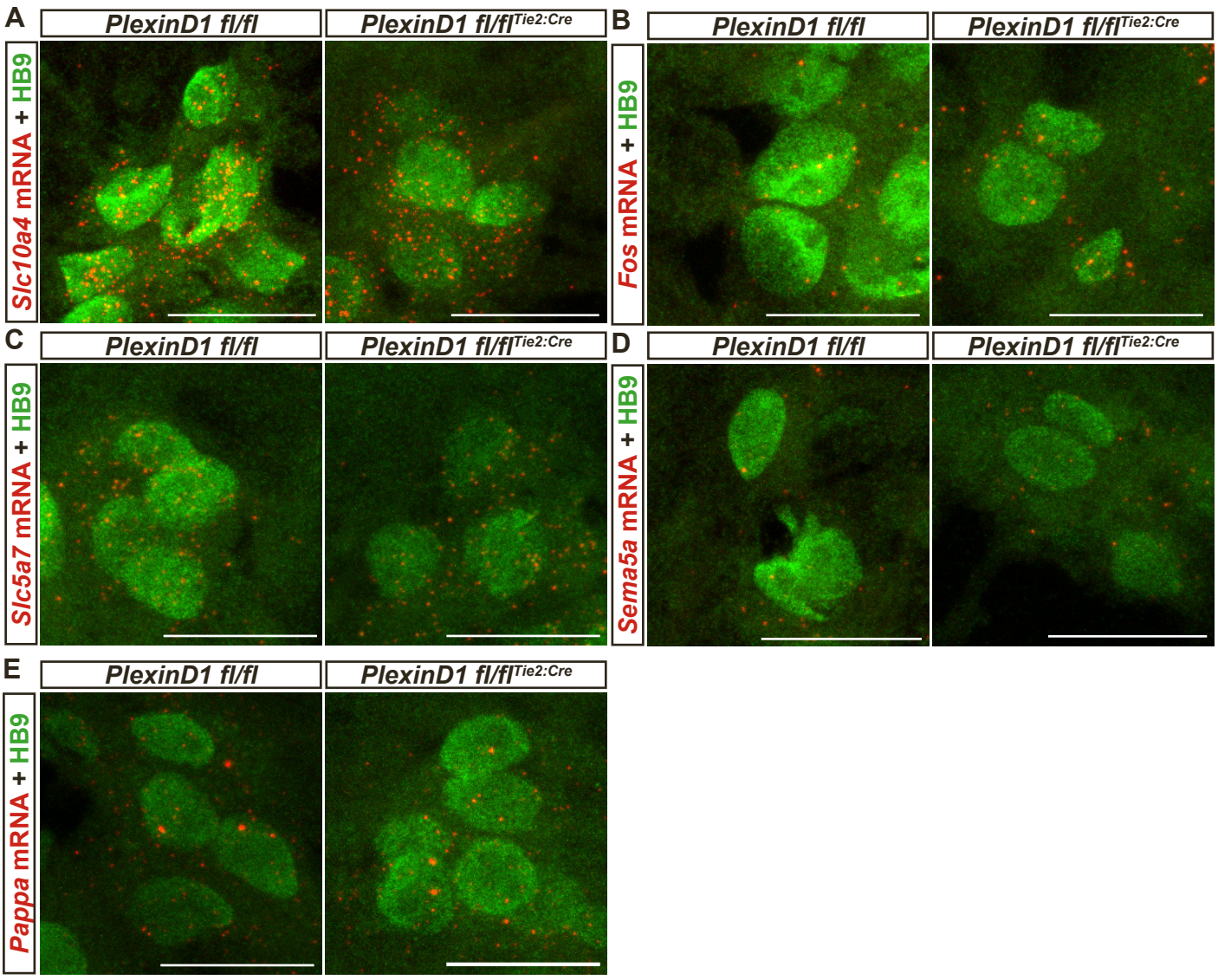

Fig. Sup. 9 - Related to Figure 6

Supplementary figure legends

Supplementary Figure 1. Predicted interactions between ECs and neural cells, and *PlexinD1* and *Nrp1* expression, related to figure 1.

(A) Graph showing the predicted interactions between the different cell types.

(B) Top five signaling pathways used between the cell types and the total number of interactions for each pathway.

(C-F) Graphs showing the predicted interactions between cell types using (C) Notch signaling, (D) Epha signaling, (E) Laminin signaling, and (F) Jam signaling.

(G-H) Temporal plot of the percentage of ECs expressing *PlexinD1* (G) and the average number of *PlexinD1* reads in ECs (H) between E9.5 to E13.5, using previously published single-cell RNAseq data (Delile, Rayon et al. 2019).

(I) Representative images for *PlexinD1* ISH between E9.5 and E12.5. *PlexinD1* mRNA is expressed only in ECs at all the SC levels. Scale bars 100 µm.

(J) Predicted expression of *Nrp1* in the different cell types between E9.5 to E11.5, using previously published single-cell RNAseq data (Delile, Rayon et al. 2019).

(K-L) Temporal plot of the percentage of ECs expressing *Nrp1* (K) and the average number of *Nrp1* reads in ECs (L) between E9.5 to E13.5, using previously published single-cell RNAseq data (Delile, Rayon et al. 2019).

(M) Representative images of RNAscope Multiplex Fluorescent Assay using *Nrp1* probe combined with staining for ECs ($IsoB4^+$). Inset shows higher magnification of vessels surrounding the MN column. Blue arrowheads point at *Nrp1* dots within ECs. Scale bar 100 µm for low magnification and 25 µm for higher magnifications.

Supplementary Figure 2. *Sema3C* is expressed in MNs during spinal cord development, related to figure 1.

(A) Representative images of *Sema3C in situ* hybridization (ISH) at brachial and thoracic level between E11.5 and E12.5. Scale bars 100 µm.

(B-C) Percentage of MNs expressing *Sema3C* (B) and the average number of (C) *Sema3C* reads in MNs over the indicated developmental times, using previously published single-cell RNAseq data (Delile, Rayon et al. 2019).

(D) Predicted expression of *Sema3C* in the different MN columns using previously published single-cell RNAseq data (Delile, Rayon et al. 2019).

(E) Representative RNAscope assay for the negative control *Dapb,* showing background staining prevenient from erythrocytes. The inset shows a higher magnification of MN column. Scale bars 100 µm.
(F) Schematic representation of MN clustering and positioning at brachial and thoracic levels of the spinal cord at E11.5.
(G) Representative images of RNAscope assay using *Sema3C* probe combined with staining for MN columns (LMCl - red circle, Isl1/2^{-}Foxp1^{+}; LMCm - yellow circle, Foxp1^{+}Isl1/2^{+}; MMC – green circle, Foxp1^{-}Isl1/2^{+}). Scale bars 100 µm.

Supplementary Figure 3. Knockdown of *PlexinD1* and *Nrp1* in ECs results in increased HBMECs tubes contacting MN explants, related to figure 2.
(A) Relative *PlexinD1* mRNA expression in HBMECs upon transfection with siRNA PlexinD1 (HBMECs-PlexinD1-KD), normalized to siRNA Ctrl (HBMECs-Control) (n=9 siRNA Ctrl, n=9 siRNA PlexinD1, from two independent experiments; parametric distribution, two tailed unpaired Student's t-test.).
(B) Quantification of MN explant size from BL6 WT embryos used for the tube touching assay (data are normalized to Control; n=72 explants cultured with HBMECs-Control, n=77 explants cultured with HBMECs-PlexinD1-KD, from two independent litters; parametric distribution, two tailed unpaired Student's t-test).
(C) Relative *Nrp1* mRNA expression in HBMECs upon transfection with siRNA Nrp1 (HBMECs-Nrp1-KD), normalized to siRNA Ctrl (HBMECs-Control) (n=10 siRNA Ctrl, n=10 siRNA Nrp1, from two independent experiments; parametric distribution, two tailed unpaired Student's t-test.).
(D) Representative images of the tube "touching" assay showing HBMEC-Control and HBMECs-Nrp1-KD tubes touching MN explants. Red arrowheads indicate contacts between HBMEC tubes and explants. Scale bars 1000 µm.
(E) Quantification of the number of either HBMECs-Control or HBMECs-Nrp1-KD tubes touching MN explants, normalized to the explant perimeter (n=37 explants siRNA Ctrl, n=28 explants siRNA Nrp1, from 2 independent litters, parametric distribution, two tailed unpaired Student's t-test).
(F) Quantification of MN explant size from BL6 WT embryos used for the tube touching assay (data are normalized to Control; n=37 explants siRNA Ctrl, n=28 explants siRNA Nrp1, from 2 independent litters, parametric distribution, two tailed unpaired Student's t-test).

All data shown as mean ± SD.

Supplementary Figure 4. PlexinD1 KO and *PlexinD1 fl/fl*$^{Tie2:Cre}$, but not *Sema3C fl/fl*$^{Olig2:Cre}$, show increased total spinal cord vascularization, related to figure 2, 3 and 4.

(A) Representative images at brachial level of *PlexinD1* ISH in *PlexinD1* WT and KO embryos at E11.5 to confirm successful global *PlexinD1* deficiency. Scale bars 100 μm.

(B) Quantification of BV density in the total SC of *PlexinD1* WT and KO embryos at E11.5. n=6 PlexinD1 WT, n=5 PlexinD1 KO, from two independent litters; parametric distribution, two tailed unpaired Student's t-test.

(C) Representative images at thoracic level of ISH for *PlexinD1* in *PlexinD1 fl/fl* and *PlexinD1 fl/fl*$^{Tie2:Cre}$ embryos at E11.5 to confirm successful *PlexinD1* knockdown in ECs. Scale bars 100 μm.

(D) Quantification of BV density in the total SC of *PlexinD1 fl/fl* and *PlexinD1 fl/fl*$^{Tie2:Cre}$ embryos at E11.5. n=4 *PlexinD1 fl/fl*, n=6 *PlexinD1 fl/fl*$^{Tie2:Cre}$, from two independent litters; parametric distribution, two tailed unpaired Student's t-test.

(E) Representative image at thoracic level of ISH for *Sema3C* in *Sema3C fl/fl* and *Sema3C fl/fl*$^{Olig2:Cre}$ embryos at E11.5 to confirm successful and specific removal of *Sema3C* in MNs (black arrows) but not roof plate (red arrow). Scale bars 100 μm.

(F) Quantification of the explant sizes used from *Sema3C fl/fl* and *Sema3C fl/fl*$^{Olig2:Cre}$ E11.5 embryos (normalized to control littermates), n=40 explants *Sema3C fl/fl*, n=125 explants *Sema3C fl/fl*$^{Olig2:Cre}$, from two independent litters; parametric distribution, two tailed unpaired Student's t-test.

(G) Quantification of BV density in the total spinal cord of *Sema3C fl/fl* and *Sema3C fl/fl*$^{Olig2:Cre}$ embryos at E11.5. n=5 *PlexinD1 fl/fl*, n=6 *PlexinD1 fl/fl*$^{Tie2:Cre}$, from two independent litters; parametric distribution, two tailed unpaired Student's t-test.

All data shown as mean ± SD.

Supplementary Figure 5. *Sema3E* KO embryos do not show MN column vascularization defects , related to figure 4.

(A) Scheme of the different spinal cord levels in a rostral to caudal axis.

(B) ISH for *Sema3E* in the developing spinal cord of WT embryos from E10.5 to E12.5 and at brachial and thoracic levels. Scale bars 100 μm.

(C) Representative image at brachial level of ISH for *Sema3E* in *Sema3E* WT and KO embryos at E11.5 to confirm successful global deletion of *Sema3E* (green arrowheads - MNs, blue arrowheads - FP).
(D) Representative images of spinal cord sections stained for BV (IsoB4^{+}) and MNs (Isl1/2^{+}) in *Sema3E* WT and KO embryos at E11.5. Insets show higher magnifications of MN columns. Scale bars 100 µm.
(E-G) Quantification of BV density in MNs at brachial level (E), at brachial and thoracic levels together (F), and BV density in the total spinal cord (G) of *Sema3E* WT and KO embryos at E11.5. n=5 *Sema3E* WT, n=7 *Sema3E* KO, from two independent litters; parametric distribution, two tailed unpaired Student's t-test.
All data shown as mean ± SD.

Supplementary Figure 6. Premature MN vascularization does not lead to defects in MN area and MN clustering, nor to defects in the position of the MEP, related to figure 5.
(A-C) Quantification of the ratio between MN area and total SC area in *PlexinD1* WT and KO embryos (A), *PlexinD1 fl/fl* and *PlexinD1 fl/fl*$^{Tie2:Cre}$ embryos (B), and *Sema3C fl/fl* and *Sema3C fl/fl*$^{Olig2:Cre}$ embryos (C) at E11.5. n=6 *PlexinD1 WT*, n=6 *PlexinD1 KO*; n=4 *PlexinD1 fl/fl*, n=6 *PlexinD1 fl/fl*$^{Tie2:Cre}$; n=5 *Sema3C fl/fl*, n=6 *Sema3C fl/fl*$^{Olig2:Cre}$, from two independent litters; parametric distribution, two tailed unpaired Student's t-test.
(D) Immunostaining shows the localization of the different MN clusters at brachial level in *PlexinD1 fl/fl* and *PlexinD1 fl/fl*$^{Tie2:Cre}$ embryos. MN clustering into the medial division of the lateral motor column (LMCm, Isl1/2+ and FoxP1+, yellow dotted outline), lateral division of lateral motor column (LMCl, FoxP1+, red dotted outline), and medial motor column (MMC, Isl1/2+, black dotted outline) is not affected in *PlexinD1 fl/fl*$^{Tie2:Cre}$ embryos. Scale bars 100 µm.
(E) Scheme representation to illustrate how the distance from the midline to the most ventral exit point is calculated.
(F-G) Quantification of the distance from the midline to the most ventral exit point (F), and the distance from the midline to the average position of the exiting motor axon bundles (G) in *PlexinD1 fl/fl* and *PlexinD1 fl/fl*$^{Tie2:Cre}$ embryos. n=4 *PlexinD1 fl/fl*, n=6 *PlexinD1 fl/fl*$^{Tie2:Cre}$, from two independent litters; parametric distribution, two tailed unpaired Student's t-test.

(H-I) Quantification of the distance from the midline to the most ventral exit point (H) and the distance from the midline to the average position of the exiting motor axon bundles (I) in *Sema3C fl/fl* and *Sema3C fl/fl*$^{Olig2:Cre}$ embryos at E11.5. n=5 *Sema3C fl/fl*, n=6 *Sema3C fl/fl*$^{Olig2:Cre}$, from two independent litters; parametric distribution two tailed unpaired Student's t-test.

(J) Representative images of 300 µm thick sections at thoracic level co-labeled for blood vessels (IsoB4) and MN axons (neurofilament M) exiting the spinal cord in *PlexinD1 fl/fl* and *PlexinD1 fl/fl*$^{Tie2:Cre}$ embryos at E11.5. Scale bars 100 µm.

All data shown as mean ± SD.

Supplementary Figure 7. Afferent inputs to MNs are not affected in *PlexinD1 fl/fl*$^{Tie2:Cre}$ embryos, related to figure 6.

(A) Quantification of the number of MNs (HB9^{+}) per SC section at E18.5 in *PlexinD1 fl/fl* and *PlexinD1 fl/fl*$^{Tie2:Cre}$ embryos, normalized to control littermates. n=7 *PlexinD1 fl/fl*, n=6 *PlexinD1 fl/fl*$^{Tie2:Cre}$, from two independent litters; parametric distribution, two tailed unpaired Student's t-test.

(B) Quantification of the MN soma size at E18.5 in *PlexinD1 fl/fl* and *PlexinD1 fl/fl*$^{Tie2:Cre}$ embryos, normalized to control littermates. n=7 *PlexinD1 fl/fl*, n=6 *PlexinD1 fl/fl*$^{Tie2:Cre}$, from two independent litters; parametric distribution, two tailed unpaired Student's t-test.

(C) Quantification of the number of MNs (HB9^{+}) at thoracic levels at E18.5 in *PlexinD1 fl/fl* and *PlexinD1 fl/fl*$^{Tie2:Cre}$ embryos, normalized to control littermates. n=7 *PlexinD1 fl/fl*, n=6 *PlexinD1 fl/fl*$^{Tie2:Cre}$, from two independent litters; parametric distribution, two tailed unpaired Student's t-test.

(D-E) Quantification of the number of MNs (HB9^{+}) at lumbar levels at E18.5 in the MMC (D) and LMC (E) columns in *PlexinD1 fl/fl* and *PlexinD1 fl/fl*$^{Tie2:Cre}$ embryos, normalized to control littermates. n=4 *PlexinD1 fl/fl*, n=4 *PlexinD1 fl/fl*$^{Tie2:Cre}$, from two independent litters; parametric distribution, two tailed unpaired Student's t-test.

(F) Quantification of the MN column area at thoracic levels at E18.5 in *PlexinD1 fl/fl* and *PlexinD1 fl/fl*$^{Tie2:Cre}$ embryos, normalized to control littermates. n=7 *PlexinD1 fl/fl*, n=6 *PlexinD1 fl/fl*$^{Tie2:Cre}$, from two independent litters; parametric distribution, two tailed unpaired Student's t-test.

(G-H) Quantification of the MMC (G) and LMC (H) column areas at lumbar levels at E18.5 in *PlexinD1 fl/fl* and *PlexinD1 fl/fl*$^{Tie2:Cre}$ embryos, normalized to control

littermates. n=6 *PlexinD1 fl/fl*, n=6 *PlexinD1 fl/fl*$^{Tie2:Cre}$, from two independent litters; parametric distribution, two tailed unpaired Student's t-test.

(I) Schematic representation of the procedure for dorsal root tracing with NeuroDiI.

(J) Representative images of coronal sections from E18.5 thoracic level spinal cords from *PlexinD1 fl/fl* and *PlexinD1 fl/fl*$^{Tie2:Cre}$ traced with NeuroDiI. Red arrowheads indicate the major proprioceptive descending bundle as well as its two main secondary branches. Scale bar 200 μm.

(K) Scheme illustrating the procedure to obtain the angles for the major proprioceptive descending bundle (α) and its main secondary branches (β and χ) as shown in (J).

(L) Quantification of (J). Average angle for (α, β and χ). n=20 *PlexinD1 fl/fl* and n=27 *PlexinD1 fl/fl*$^{Tie2:Cre}$ spinal cord sections were analyzed from three independent experiments; Comparison in ordinary 1-way ANOVA.

(M) Schematic representation of MN connectivity. MNs receive signal inputs from sensory neurons, cholinergic, inhibitory, and excitatory interneurons (IN).

(N) Images of ventral spinal cords immunostained for MNs (HB9^{+}) and cholinergic inputs (VAChT^{+}) in *PlexinD1 fl/fl* and *PlexinD1 fl/fl*$^{Tie2:Cre}$ embryos at E18.5. Scale bars 100 μm.

(O) Quantification of the cholinergic synaptic density contacting MNs in *PlexinD1 fl/fl* and *PlexinD1 fl/fl*$^{Tie2:Cre}$ embryos at E18.5. Data normalized to the control. n=7 PlexinD1 fl/fl, n=6 PlexinD1 fl/fl$^{Tie2:Cre}$, from two independent litters; parametric two tailed unpaired Student's t-test.

(P) Images of ventral spinal cord immunostained for MNs (HB9^{+}), MN soma (HB9+ and Chat+), and inhibitory inputs (VGAT^{+}) in *PlexinD1 fl/fl* and *PlexinD1 fl/fl*$^{Tie2:Cre}$ embryos at E18.5. Scale bars 100 μm.

(Q) Quantification of inhibitory synaptic density connecting to MNs in *PlexinD1 fl/fl* and *PlexinD1 fl/fl*$^{Tie2:Cre}$ embryos at E18.5, normalized to control littermates. n=7 PlexinD1 fl/fl, n=6 PlexinD1 fl/fl$^{Tie2:Cre}$, from two independent litters; parametric distribution, two tailed unpaired Student's t-test.

All data shown as mean ± SD.

Supplementary Figure 8. Altered transcription of MN terminal differentiation markers and functional genes in *PlexinD1 fl/fl*$^{Tie2:Cre}$ embryos at E18.5, related to figure 6.

(A-D) Representative images of RNAscope for *Glra2 (A), Nrg1 (B), Slc18a3 (C), and Mcam (D)* co-stained with HB9 in *PlexinD1 fl/fl* and *PlexinD1 fl/fl*$^{Tie2:Cre}$ embryos. Scale bar 25 μm.

(E-F) Quantification of the number of RNAscope dots for the different genes per HB9^{+} nucleus in the MMC (E) and LMC (F) columns. Data normalized to control littermates. n=5 *PlexinD1 fl/fl*, n=4 *PlexinD1 fl/fl*$^{Tie2:Cre}$, from two independent litters; multiple Student's t-test.

(G) Representative images of the intercostal muscles at E18.5 stained to show intercostal innervation (Neurofilament M + Synaptophysin), AchR^{+} clusters (α-bungaratoxin), and BVs (IsoB4) in *PlexinD1 fl/fl* and *PlexinD1 fl/fl*$^{Tie2:Cre}$ embryos. Scale bars 100 μm.

(H) Quantification of the branching density of phrenic nerve at E18.5 in *PlexinD1 fl/fl* and *PlexinD1 fl/fl*$^{Tie2:Cre}$ embryos. n=4 *PlexinD1 fl/fl*, n=4 *PlexinD1 fl/fl*$^{Tie2:Cre}$, from two independent litters; parametric distribution, two tailed unpaired Student's t-test.

All data shown as mean ± SD.

Supplementary Figure 9. Gene expression analysis via RNAscope in MNs of *PlexinD1 fl/fl* and *PlexinD1 fl/fl*$^{Tie2-}$*Cre* E18.5 embryos, related to figure 6.

(A-E) Representative images of RNAscope for *Slc10a4 (A), Fos (B), Slc5a7 (C), Sema5a* (D) and *Pappa* (E) co-stained with HB9 in *PlexinD1 fl/fl* and *PlexinD1 fl/fl*$^{Tie2:Cre}$ embryos. Scale bar 25 μm.